Open Veterinary Journal, (2025), Vol. 15(1): 69-84
ISSN: 2226-4485 (Print)
ISSN: 2218-6050 (Online)

Research Article
DOI: *10.5455/OVJ.2025.v15.i1.6*

Submitted: 18/10/2024 Accepted: 27/12/2024 Published: 31/01/2025

Exploring the SARS-CoV-2 spike protein destabilizer toxin from the scorpion, spider, and wasp group of toxins as a promising candidate for the identification of pharmacophores against viral infections

Mousa O. Germoush[1]*, Maged Fouda[1], Mohammad J. S. Mantargi[2], Moustafa Sarhan[3,4], Barakat M. AlRashdi[1], Diaa Massoud[1], Ahmed E. Altyar[5,6] and Mohamed M. Abdel-Daim[2,7]

[1]*Biology Department, College of Science, Jouf University, Sakaka, Saudi Arabia*
[2]*Department of Pharmaceutical Sciences, Pharmacy Program, Batterjee Medical College, Jeddah, Saudi Arabia*
[3]*Department of Biomedical Sciences, College of Clinical Pharmacy, King Faisal University, Al Hofuf, Saudi Arabia*
[4]*Department of Zoology, Faculty of Science, Al-Azhar University, Assuit, Egypt*
[5]*Department of Pharmacy Practice, Faculty of Pharmacy, King Abdulaziz University, Jeddah, Saudi Arabia*
[6]*Pharmacy Program, Batterjee Medical College, Jeddah, Saudi Arabia*
[7]*Pharmacology Department, Faculty of Veterinary Medicine, Suez Canal University, Ismailia, Egypt*

ABSTRACT

Background: The SARS-CoV-2 virus is the infectious agent that causes coronavirus illness (COVID-19). The majority of virus-infected individuals will recover without the need for special care after experiencing mild-to-moderate respiratory symptoms. Some people, nevertheless, will get quite sick and need medical help. The choice of COVID-19 treatment should be made individually. The severity of the illness and the chance that it will worsen will determine the decision. Therefore, developing more potent medications is always a primary goal. Finding more effective drugs is a top priority. In this regard, natural animal toxins, such as toxin derived from scorpions, spiders, and wasps, have been found to include compounds that have significant therapeutic properties. Specifically, targeting the spike protein which acts as a gateway for the vires to enter the human or animal cells.

Aim: This study focuses on the ability of toxins to destabilize the spike protein of the SARS-CoV-2 virus, which is responsible for the SARS-CoV-2 pandemic.

Methods: The active protein structure of the SARS-CoV-2, the toxins chosen obtained from the RCSB-protein data bank (PDB), and the molecular structures of toxins that were not proteins were either obtained from PubChem or downloaded as computer structure models from RCSB-PDB. Using molecular docking software such as "PyRx," analyzers such as "BIOVIA-Discovery studios" and "Pymol," and various techniques, the evaluation of the interactions between the spike protein and toxin was performed, to find possible pharmacophores that might serve as a foundation for upcoming medication development. The protein-ligand complex was put to test through the molecular dynamic (MD) simulation via visual molecular dynamics /nanoscale molecular dynamics application to determine the complex stability.

Results: The current research findings reveal intriguing binding affinities and interaction patterns between the toxin and the SARS-CoV-2 spike protein, where the complex was identified to be stable throughout the study resembling the cellular conditions via MD simulations. We discuss the implications of these interactions and how they might interfere viral infection and entry.

Conclusion: The current study sheds light on a promising avenue for the development of antiviral therapies, leveraging natural venoms as a source of inspiration for pharmacophore-based drug discovery opposing viral infections.

Keywords: SARS-CoV-2, Scorpions toxins, Spider toxins, Wasps toxins, Spike protein, Molecular docking, Pharmacophore.

Introduction

Based on the SARS-CoV-2 pandemic and its fatal effects explored globally, various sets of research were planned and put into effect to identify the primary route and mechanism of viral infection. Similarly, the current research planned to focus primarily on the spike protein of the virion of the coronavirus, which is designated as the primary route of entry into the healthy human

***Corresponding Author:** Mousa O. Germoush. Biology Department, College of Science, Jouf University, Sakaka, Saudi Arabia. Email: *mogermoush@ju.edu.sa*

cells. However, the basic component of an infectious virus is made up of nucleic acid that is enveloped by an exterior protein shell known as virion. In 2003, as a result of the SARS-CoV outbreak in southern China and its broad incidence, more than 8,000 persons were affected, and 774 fatalities were recorded, according to the World Health Organization (WHO). A second outbreak of acute respiratory illness was detected in Saudi Arabia in 2012, and MERS-CoV was found to be the epidemic's cause. The death rate was around 35%, according to the reports that were released (Mudenda *et al.*, 2021a).

Since then, several studies have been done targeting different kinds of the virus including the corona spike protein, which is the virus' point of attachment to enter the host cells. On the other hand, it is also recognized that the toxins made by scorpions, spiders, wasps, bacteria, fungi, and plants specifically target particular cellular targets and disrupt regular cellular processes. The potential interactions between the corona spike protein and other toxins are examined in this research paper using molecular docking methods to understand the mode of action of these toxins and find possible therapeutic targets to fight not only SARS-CoV-2 but also other virus-mediated disorders (Mudenda *et al.*, 2021b).

The WHO classified SARS-CoV-2 to be a pandemic brought on by SARS-CoV-2 in March, 2020. The SARS-CoV-2 primarily affects the cells of the human respiratory system. However, recent research has shown that the virus affects the cells of the eyes, liver, kidney, pancreas, and brain. About 79% and 50% of the SARS-CoV-2 viruses are comparable to the SARS and MERS viruses. A global crisis has resulted from the widespread prevalence of SARS-CoV-2 due to the high transmission strength and complexity of SARS-CoV-2 therapy compared to MERS-CoV and SARS-CoV, and it is essential to stop the disease spread (Salahshoori *et al.*, 2021).

In this regard, the results of the current study emphasize the value of all encompassing strategy to fight infectious diseases, including the investigation of therapeutic alternatives to conventional antiviral medications. The novelty of the study includes determination of the anti-corona activity of natural toxins produced by the living organisms such as scorpion, spider, and wasp and evaluation of the entry inhibition for coronavirus into the healthy human cells through molecular dynamic (MD) simulations and molecular docking.

Materials and Methods

Target and ligand-protein selection

The 3D confirmers of the coronavirus spike protein's electron microscopy, NMR, and crystallographic coordinates, scorpion toxins (n = 8), spider toxins (n = 3), and wasp toxin (n = 1) structures were provided from the protein data bank (PDB) with the following properties: coronavirus spike protein PDB IDs: 7R40 (resolution: 2.9 Å) (Du *et al.*, 2022), scorpion toxin (st1): PDB ID: 5XA6 (Meng *et al.*, 2020), scorpion toxin (st2): PDB ID: 7X41 (resolution: 1.15 Å) (Arzamasov *et al.*, 2014), scorpion toxin (st3) PDB ID: 1CZ6 (Mandard *et al.*, 1999), scorpion toxin (st4) PDB ID: 5TOD (resolution: 2.96 Å) (Lees *et al.*, 2017), spider toxin (st5) PDB ID: 6CL3 (Reis *et al.*, 2018), spider toxin (st6) PDB ID: POC2VO-F1 (computed model) (Vassilevski *et al.*, 2010), spider toxin (st7) PDB ID: A9QQ26-F1 (computed model) (Vassilevski *et al.*, 2010), wasp toxin (st8) PDB ID: 1A13) ((Kusunoki *et al.*, 1998), scorpion toxin (BL1): PDB ID: BL1, scorpion toxin (BL2): PDB ID: BL2, scorpion toxin (BL3): PDB ID: BL3, scorpion toxin (BL4): PDB ID: BL4, and scorpion toxin (SMP): PDB ID: SMP.

The desired proteins were prepared by removing the pre-bonded ligands and water molecules from the structure, and then the polar hydrogens were added as needed to ensure that the proteins and ligands (toxins) were sorted for further processing. Drug possibilities for all ligands were evaluated by Lipinski's rule of five. Molecular body weight < 500 Da, up to 5 hydrogen bond donors 10 as hydrogen bond acceptor and logP (octanol–water distribution) factor must not exceed 5.

Protein-ligand interaction

An Autodock vina integrated *PyRx Python prescription 0.8* (*https://pyrx.sourceforge.io/*) (Dallakyan and Olson, 2015) application was preferred for virtual screening and molecular docking of 3D structures of BL1, BL2, BL3, BL4, and SMP which were obtained in *SDF* format was selected against coronavirus spike protein where the filtered protein structure was loaded and converted into macromolecule. The ligand was added from an external compatible file into the same interface after energy minimizing by applying a universal force field and converting it into a *pdbqt* file through *openbabel*. As both the files appeared in the interface, the vina wizard was started and the grid was constructed for the protein basing up the active sites and for those where the previous data regarding the grid dimensions was not available complete protein was selected as maximized grid. The affinity scores were obtained after running the hit and the final best docked model was saved as a *pdb* file for further analysis (Odoemelam *et al.*, 2022).

The analysis of the molecular docking models was performed employing *BIOVIA-Discovery studios visualizer v.21.1.0.20298* (https://discover.3ds.com/discovery-studio-visualizer-download) where the *pdb* file obtained was loaded and the 2D structure of the interactive amino acids with their hydrogen and electrostatic bond lengths were noticed (BIOVIA, 2020).

Protein-protein interactions: Cluspro2

Cluspro2 (https://cluspro.bu.edu/login.php), which runs through an automated algorithm, was preferred for protein–protein docking (Kozakov *et al.*, 2013, 2017; Vajda *et al.*, 2017). The spike protein *pdb* files and

various ligand proteins were uploaded into the server of *cluspro2* (Vadja *et al.*, 2017). The results of the protein–protein docking were obtained as *balanced, electrostatic favored, hydrophobic favored, and Van der waals and electrostatic cluster scores*. As the data expressed in negative values, the highest negative score considered as the lowest score. The molecular interacted models were analyzed through *ligplot plus v2.2* (https://www.ebi.ac.uk/thornton -srv/software/LigPlus/download.html) (Laskowski and Swindells, 2011) and pymol (https://pymol.org/2/) (Schrödinger, 2015) which revealed the length of H-bonds in addition to interactive amino acids in the interactive sites of the two proteins. The results of the study expressed in Tables (1 and 2) and Figures (1–13).

Molecular dynamic (MD) simulation of the ligand–protein complex

The ligand (Wasp toxin-Mastoparan) with the best affinity scores was selected to perform the MD simulation studies. Visual molecular dynamics (VMD) https://www.ks.uiuc.edu/Research/vmd/ and nanoscale molecular dynamics (NAMD) https://www.ks.uiuc.edu/Research/namd/ were employed in studying the ligand effect, i.e., Wasp toxin-Mastoparan with the spike protein fragment of SARS-CoV-2. Linux operating system with NVIDIA—CUDA—GPU environment was selected for performing the simulations. NMDA and VMD were pathed in Linux supported by *tcl* and *python* script languages. After entering the commands in the command prompt of the VMD/NMDA, various *log, psf, and dcd* files were generated, later uploaded in to the VMD visual interface for the analysis of the results (Humphrey *et al.*, 1996).

Results

The rapid global spread of the coronavirus compelled researchers to look for potential treatments to stop the spread of the lethal viral infection. Finding effective medications with fewer side effects is urgently needed to combat SARS-CoV-2. Worldwide research was done to find a way to the management of SARS-CoV-2. Computer-aided virtual screening is economical and speeds up the process of getting a drug to market. According to molecular docking studies (Bansal *et al.*, 2021), lead molecules bind to the targets of SARS-CoV-2 in a specific manner. Since the viral surface spike protein (glycoproteins) plays a significant role in viral entry, it is important to assess potential drug molecules from natural sources including the toxins of selected species. The Corona cell surface spike glycoprotein is

Table 1. PyMOL analysis of "*Cluspro2*" protein–protein docking results: target proteins, corona spike protein (PDB ID: 7R40), and various toxins as ligand proteins.

Name	PDB ID	RMSD	H-bond interactions (Å units)	Amino acids of ligand-protein (in the reacted pocket)	Van der waals and electrostatic force cluster scores	Electrostatic favored—cluster scores	Hydrophobic favored—cluster scores	Balanced scoreCluster scores
1. Scorpion toxin-Bmkdfsins	5XA6	4.185	2.0–2.7	LYS 38	−349.7	−1354.9	−1464.3	−1168.4
2. Scorpion toxin-Chlorotoxin	7X41	1.837	1.8–2.8	CYS 20	−236.4	−1054.4	−1307	−1036.1
3. Scorpion toxin-Androctonin	1CZ6	8.421	1.8–2.8	THR 21	−346.3	−1420.8	−1497	−1189.6
4. Scorpion toxin-SMP 24	5TOD	11.966	1.7–2.7	GLN 82	−287.8	−1334.8	−1430.7	−1259
5. Spider toxin-Lycosin	6CL3	3.596	1.7–2.7	GLN 19	−303.5	−1010.6	−1506.4	−981.4
6. Spider toxin-Lycotoxin-L	POC2VO-F1	1.968	1.7–2.6	ASP 568	−239.9	−880.9	−1176.5	−829.4
7. Spider toxin-Allergen 5	A9QQ26-F1	5.316	1.7–2.8	THR 56	−194.6	−1096	−1544.1	−1109.4
8. Wasp toxin-Mastoparan	1A13	26.498	1.7–2.5	TYR 315	−350.1	−1451.6	−2032.4	−1416.9

Table 2. Protein–ligand docking results of "*PyRx python prescription 0.8*" and analyzed through "*BIOVIA-Discovery studios visualizer v.21.1.0.20298*": Corona spike protein (PDB ID: 7R40) as target and various toxins as ligand

Sr No	Name or Synonym	Affinity score	RMSD	Ionic or wander wall's interactions (Å units)	Hydrogen bond interactions (Å units)	Amino acids
1. Scorpion toxin-BL1 (Figure 9)	Indapamide	−7.8	0	5.16	2.19	TYR 102
2. Scorpion toxin-BL2 (Figure 10)	N-(tert-butoxy carbonyl)-L-leucine	−5	0	4.53	1.82	TRP 436, PHE 374, ASN 437, ASN 440, LEU 441, SER 438 ASN 439
3. Scorpion toxin-BL3 (Figure 11)	Biliverdin XIII ALPHA	−8.3	0	3.62	2.35	ARG 102, TRP 104, PHE 192, ILE 119, ILE 203, LEU 229, TYR 170, VAL 227, ILE 128, VAL 126, ASN 121, ARG 190, SER 172
4. Scorpion toxin-BL4 (Figure 12)	S-3a-hydroxy-5-methyl-1-phenyl-2,3,3a,4-tetrahydro-1H-pyrrolo[2,3-b] quinolin-4-one	−7.3	0	4.47, 5.46	0	TYR 102, LEU 452
5. Scorpion toxin-SMP (Figure 13)	2'-deoxy-adenosine -5'-sp-monomethyl phosphonate	−6.5	0	3.99	2.2	ASP 40, TYR 32, GLU 406, ARG 403, TYR 495, ILE 402, LYS 417, TYR 453, ILE 418, GLN 409

regarded as the most efficient therapeutic approach to limit virus entry and spread in individuals. In particular, for infectious diseases, natural products are regarded as the most significant resource for drug research and development (Alhowaish *et al.*, 2022). In recent years, 53% of FDA-approved natural product-based drugs, including antiviral agents, are of microbial origin (El Sayed *et al.*, 2020). Natural products of microbial origin are well-thought-out to be unique in terms of their chemical diversity. To investigate 13 potential toxins of scorpion, spider, and wasp origin, molecular docking studies were conducted. According to their dock score, each one of these molecules was ranked after docking against the target protein (Tables 1 and 2). The more stable binding between the target protein and the ligand/protein is indicated by the docked model with the lowest binding energy and highest binding affinity. Results from molecular docking studies explained strong interactions between 13 potential ligands (toxins) and the SARS-CoV-2 surface glycoprotein in various ligand–protein and protein–protein interactions with a specific binding affinity (docking scores). We chose all of the ligands based on their binding affinities. The visualization of structures with high dock scores using PyMOL (for protein–protein interaction) or BIOVIA-Discovery studios visualizer v.21.1.0.20298 (for protein–ligand interaction) revealed the specific amino acids involved in ligand–protein/protein–protein binding. Five chains, A, B, C, D, and G, were present in the SARS-CoV-2 surface glycoprotein (PDB ID 7R40) from SARS-CoV-2 and may interact with ligands or protein toxins (Hu *et al.*, 2021) (Tables 1 and 2).

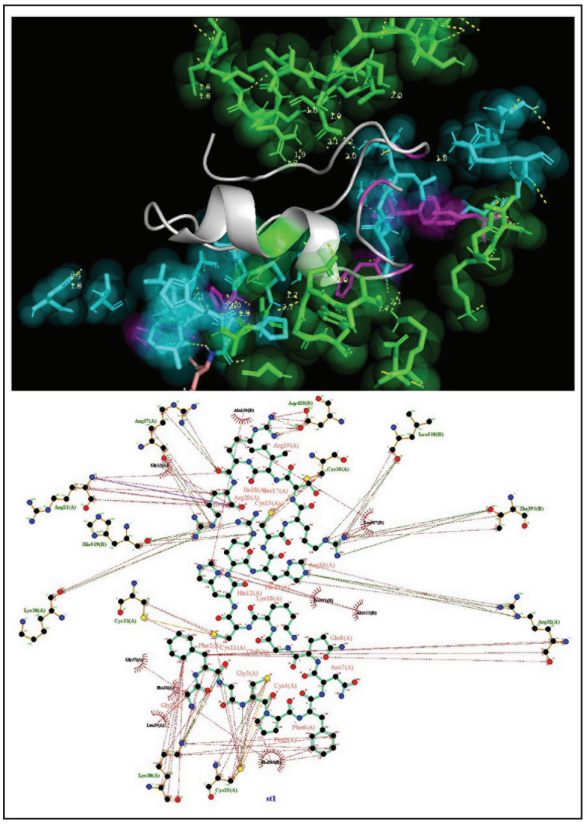

Fig. 1. Surface/glycoprotein of SARS-CoV-2 [PDB ID 7R40] with st1 (PDB ID 5XA6) (scorpion toxin)

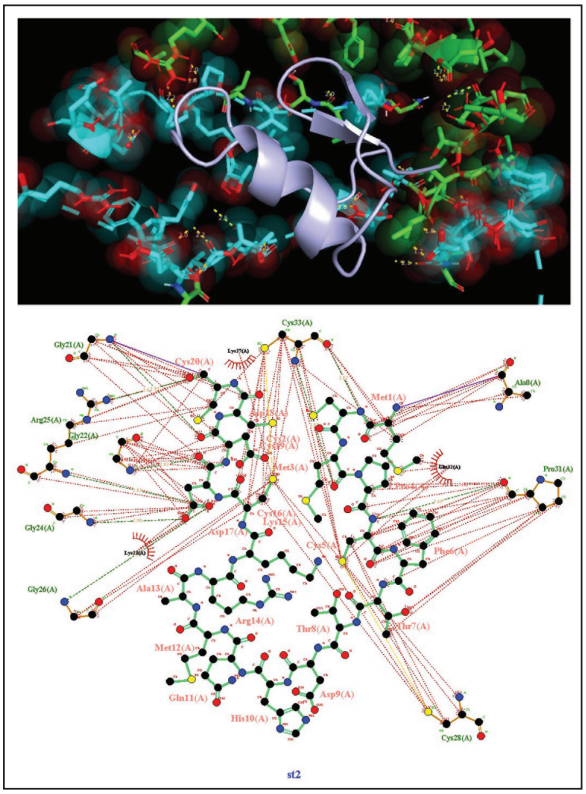

Fig. 2. Surface/glycoprotein of SARS-CoV-2 [PDB ID 7R40] with st2 (PDB ID 7X41) (scorpion toxin).

Corona spike protein images and how it interacts with different toxins from scorpion, spider, and wasp origin

a. Corona spike protein interacted with various protein toxins (PyMOL derived)

Complex of SARS-CoV-2 surface-glycoprotein–st1 (scorpion toxin 1)

The docking analysis of the SARS-CoV-2 surface glycoprotein with st1 (spider toxin 1) revealed significant binding affinities, with cluster scores of 349.7 kcal/mol for Van der waals and electrostatic force, −1354.9 for electrostatic favored /cluster scores, −1464.3 for hydrophobic favored/cluster scores, and balanced score/cluster scores of −1168.4. The ARG 20 of chain A of st1 and the LYS 38 of chain A of SARS-CoV-2 surface glycoprotein form hydrogen bonds with the smallest distance of 2.685 Å as a result of this protein interaction (Fig. 1) (Table 1).

Complex of SARS-CoV-2 surface glycoprotein and st2 (scorpion toxin 2)

The docking analysis of the SARS-CoV-2 surface glycoprotein with st2 (spider toxin 2) revealed significant binding affinities, with cluster scores of −236.4 kcal/mol for Van der waals and electrostatic force, −1054.4 for electrostatic favored /cluster scores, −1307 for hydrophobic favored/cluster scores, and balanced score/cluster scores of −1036.1. This protein interaction resulted in hydrogen bonds between CYS 20 of chain A of SARS-CoV-2 surface glycoprotein and ARG 25 of chain A of st2, with the shortest distance being 2.627 Å (Fig. 2, Table 1).

Complex of SARS-CoV-2 surface-glycoprotein–st3 (scorpion toxin 3)

The docking analysis of the SARS-CoV-2 surface glycoprotein with st3 (scorpion toxin 3) revealed significant binding affinities with cluster scores of −346.3 kcal/mol for Van der waals and electrostatic forces, −1420.8 kcal/mol for electrostatic favored interactions, −1497 kcal/mol for hydrophobic favored interactions, and −1189.6 kcal/mol for the balanced score. The interaction is stabilized by a hydrogen bond between LYS19 of chain A in st3 and THR21 of chain A in the SARS-CoV-2 surface glycoprotein, with a shortest bond distance of 2.508 Å, as shown in Fig. 3 and detailed in Table 1.

Complex of SARS-CoV-2 surface-glycoprotein–st4 (scorpion toxin 4)

The docking of the SARS-CoV-2 surface glycoprotein with st4 (scorpion toxin 4) demonstrated significant binding affinities, with cluster scores of −287.8 kcal/mol for Van der waals and electrostatic forces, −1334.8 for electrostatic favored interactions, −1430.7 for hydrophobic favored interactions, and −1259 for the balanced score. The interaction includes non-bonded

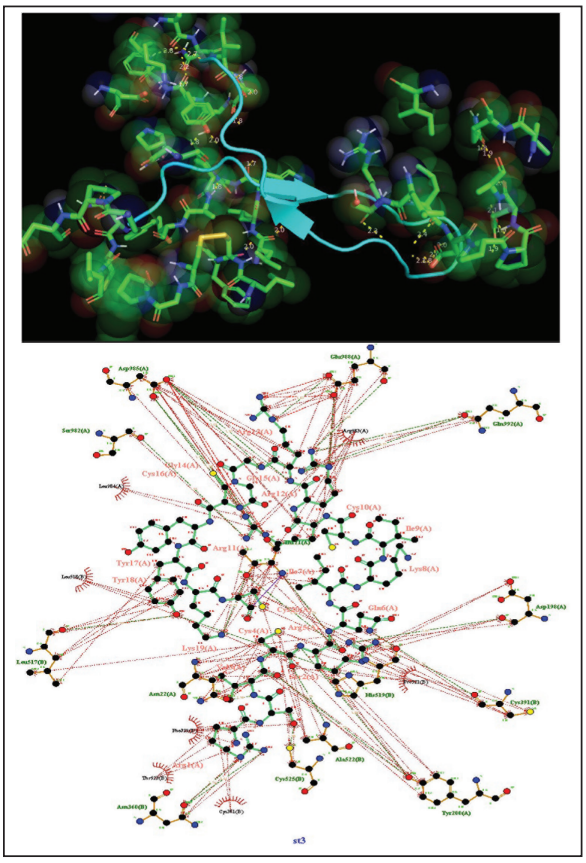

Fig. 3. Surface/glycoprotein of SARS-CoV-2 [PDB ID 7R40] with st3 (PDB ID 1CZ6) (scorpion toxin).

contacts between ILE205 of chain A in st4 and LEU203 of chain A in the SARS-CoV-2 surface glycoprotein (shortest distance: 3.578 Å), and ILE121 of chain D in st4 and GLY118 of chain D in the SARS-CoV-2 surface glycoprotein (shortest distance: 3.800 Å). Additionally, hydrogen bonding was observed between ARG19 of chain E in st4 and GLN82 of chain E in the SARS-CoV-2 surface glycoprotein, with a shortest distance of 2.717 Å. (Refer to Fig. 4 and Table 1 for details).

Complex of SARS-CoV-2 surface-glycoprotein–st5 (spider toxin 5)

The docking analysis of the SARS-CoV-2 surface glycoprotein with st5 (spider toxin 5) revealed significant binding affinities, with cluster scores of 303.5 kcal/mol for Van der waals and electrostatic forces, −1010.6 for electrostatic favored interactions, −1506.4 for hydrophobic favored interactions, and −981.4 for the balanced score. The interaction was stabilized by a hydrogen bond between LYS23 of chain A in st5 and GLN19 of chain A in the SARS-CoV-2 surface glycoprotein, with the shortest bond distance measured at 2.758 Å (Fig. 5, Table 1).

Complex of SARS-CoV-2 surface-glycoprotein–st6 (spider toxin 6)

The docking of the SARS-CoV-2 surface glycoprotein with st6 (spider toxin 6) showed significant binding affinities, with cluster scores of −239.9 kcal/mol for Van der waals and electrostatic forces, −880.9 for electrostatic favored interactions, −1176.5 for hydrophobic favored interactions, and −829.4 for the balanced score. The interaction was stabilized by

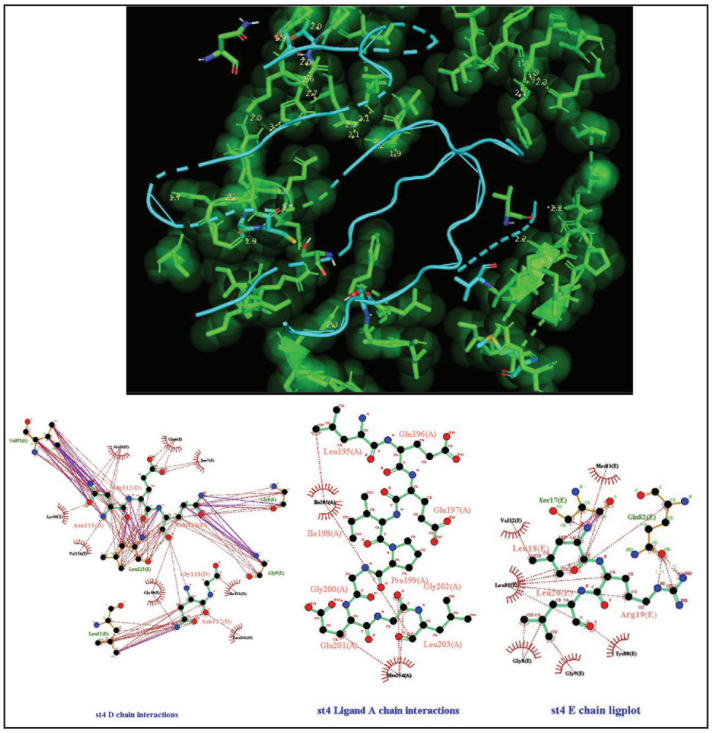

Fig. 4. Surface/glycoprotein of SARS-CoV-2 [PDB ID 7R40] with st4 (PDB ID 5TOD) (scorpion toxin).

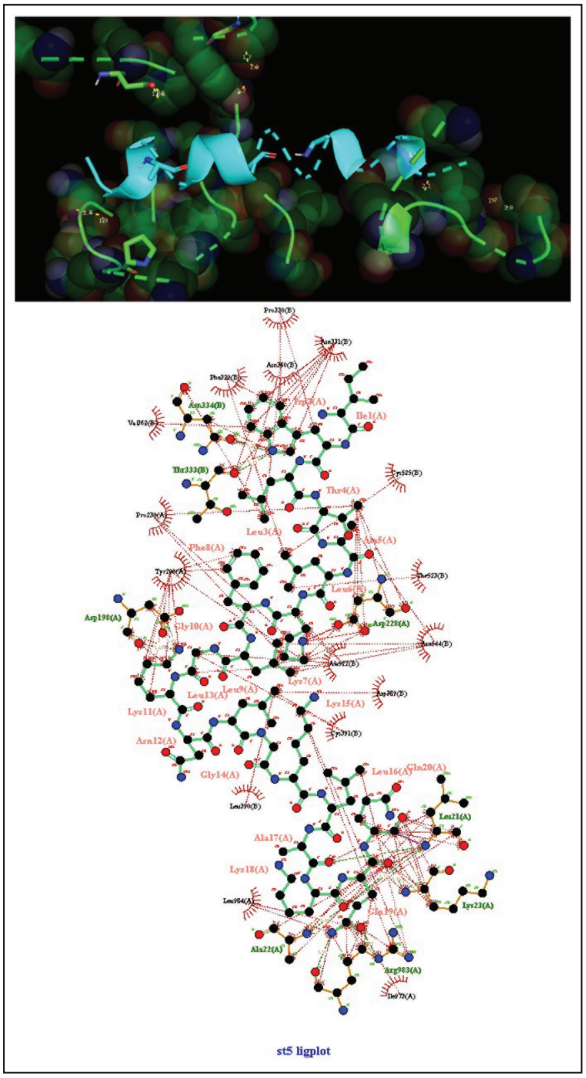

Fig. 5. Surface/glycoprotein of SARS-CoV-2 [PDB ID 7R40] with st5 (PDB ID 6CL3) (spider toxin).

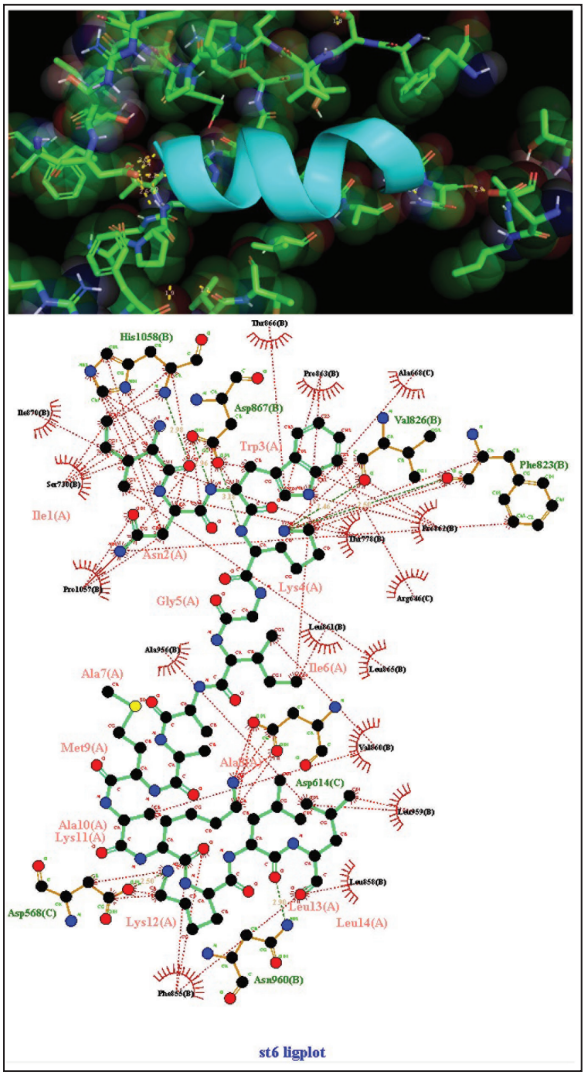

Fig. 6. Surface/glycoprotein of SARS-CoV-2 [PDB ID 7R40] with st6 (PDB ID POC2VO-F1) (spider toxin).

a hydrogen bond between LYS12 of chain A in st6 and ASP 568 of chain C in the SARS-CoV-2 surface glycoprotein, with the shortest bond distance of 2.503 Å (Fig. 6, Table 1).

Complex of SARS-CoV-2 surface-glycoprotein–st7 (spider toxin 7)

The docking of the SARS-CoV-2 surface glycoprotein with st7 (spider toxin 7) revealed significant binding affinities, with cluster scores of −194.6 kcal/mol for Van der waals and electrostatic forces, −1096 for electrostatic favored interactions, −1544.1 for hydrophobic favored interactions, and −1109.4 for the balanced score. The interaction was stabilized by a hydrogen bond between LYS13 of chain A in st7 and THR56 of chain L in the SARS-CoV-2 surface glycoprotein, with the shortest bond distance of 2.623 Å (Fig. 7, Table 1).

Complex of SARS-CoV-2 surface-glycoprotein–st8 (wasp toxin 8)

The docking of the SARS-CoV-2 surface glycoprotein with st8 (wasp toxin 8) demonstrated significant binding affinities, with cluster scores of −350.1 kcal/mol for Van der waals and electrostatic forces, −1451.6 for electrostatic favored interactions, −2032.4 for hydrophobic favored interactions, and −1416 for the balanced score. The interaction was supported by hydrogen bonds between GLY502 of chain C in st8 and TYR315 of chain A in the SARS-CoV-2 surface glycoprotein (shortest distance: 2.788 Å) and ARG54 of chain G in st8 and SER351 of chain A in the SARS-CoV-2 surface glycoprotein (shortest distance: 2.659 Å) (Fig. 8, Table 1).

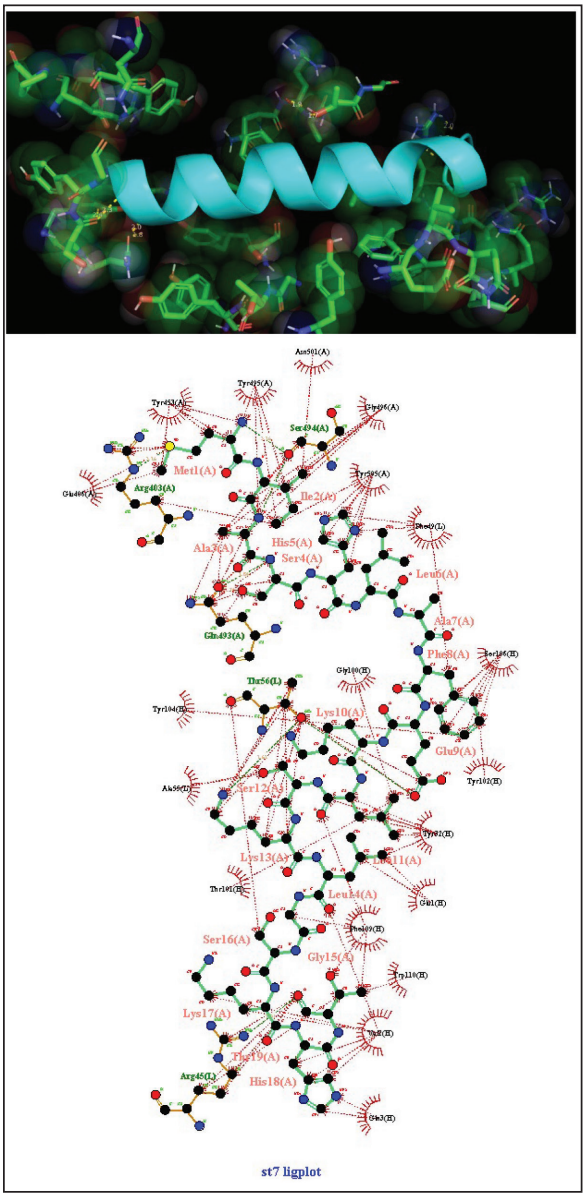

Fig. 7. Surface/glycoprotein of SARS-CoV-2 [PDB ID 7R40] with st7 (PDB ID A9QQ26-F1) (spider toxin).

b. Corona spike protein interacted with various non-protein toxins (BIOVIA-Discovery studios visualizer v.21.1.0.20298)

SARS-CoV-2 surface-glycoprotein–BL1 (scorpion toxin 9) complex

A significant binding affinity of −7.8 kcal/mol was observed during the docking of the SARS-CoV-2 surface glycoprotein against the BL1 (scorpion toxin 9) complex. This ligand interacted with the tyr 102 residue of chain E through H-bonds, and ser 494 of the C-chain acted as an unflavored donor group (Fig. 9; Table 2).

SARS-CoV-2 surface-glycoprotein–BL2 (scorpion toxin 10) complex

The docking of the SARS-CoV-2 surface-glycoprotein–BL2 (scorpion toxin 10) complex displayed a significant binding affinity of −5 kcal/mol. This ligand interacted through hydrogen bonds with asn 437, asn 440, leu 441, and asn 439 residues of chain C and pi-sigma bond with trp 104, phe 192 of C-chain and formed Van der waals interaction with asp 442, ser 438, ser 373, arg 509, and asn 434 (Fig. 10; Table 2).

SARS-CoV-2 surface-glycoprotein–BL3 (scorpion toxin 11) complex

A significant binding affinity of −8.3 kcal/mol was recorded during the docking of the SARS-CoV-2 surface glycoprotein against the BL3 (scorpion toxin 11) complex. This ligand formed Van der waals with gly 103, ile 101, phe 175, gln 173, his 207, and met 177 and interacted through H-bonds with arg 102, asn 121, ser 172, and arg 190 residues of chain B as well as pi-sigma bonds with val 126, val 227, and tyr 170 of the B-chain (Fig. 11; Table 2).

SARS-CoV-2 surface-glycoprotein–BL4 (scorpion toxin 12) complex

A significant binding affinity of −7.3 kcal/mol was observed during the docking of the SARS-CoV-2 surface-glycoprotein-BL4 (scorpion toxin 12) complex. This ligand made no H-bonds with any of the chains' residues, but it did form Van der waals interactions with the corona spike protein's glu 484, tyr 489, tyr 104, phe 490, gln 493, leu 492, ser 494, and tyr 449, as well as a pi-alkali bond with leu 452 od chain C (Fig. 12; Table 2).

SARS-CoV-2 surface-glycoprotein–SMP (scorpion toxin 13) complex

A significant binding affinity of −6.5 kcal/mol was observed during the docking of the SARS-CoV-2 surface-glycoprotein-SMP (scorpion toxin 13) complex. This ligand formed Van der waals interactions with tyr 104, leu 455, gln 493, asn 53, tyr 505, and ile 402. It also interacted through H-bonds with lys 457, tyr 32, 453, 495, and glu 406 residues of the C chain and a pi-sigma bond with ile 418 of the E chain (Fig. 13; Table 2).

MD simulations

The MD simulation showed that the ligand (Wasp toxin-Mastoparan)–protein (SARS-CoV-2 spike protein) complex had an RMSD of 0.39–0.54 and a radius of gyration (Rg) of 51.236–51.25. The potential energy and Van der Waals surface area (VSA) were also found to be 0.026-0.34 for the ligand and 0.026-0.34 for the protein. This means that the protein and ligand stayed in a stable bond during the experiment, with only minor changes in their shape. The measure of compactness exhibits almost negligible change, which also solidifies the stability of the complex; and potential energy: 5,280,507–5,280,844 and the VSA: 245,950–246,400 Reflecting the ligand-protein surface, respectively, these values clearly demonstrate the stability of the

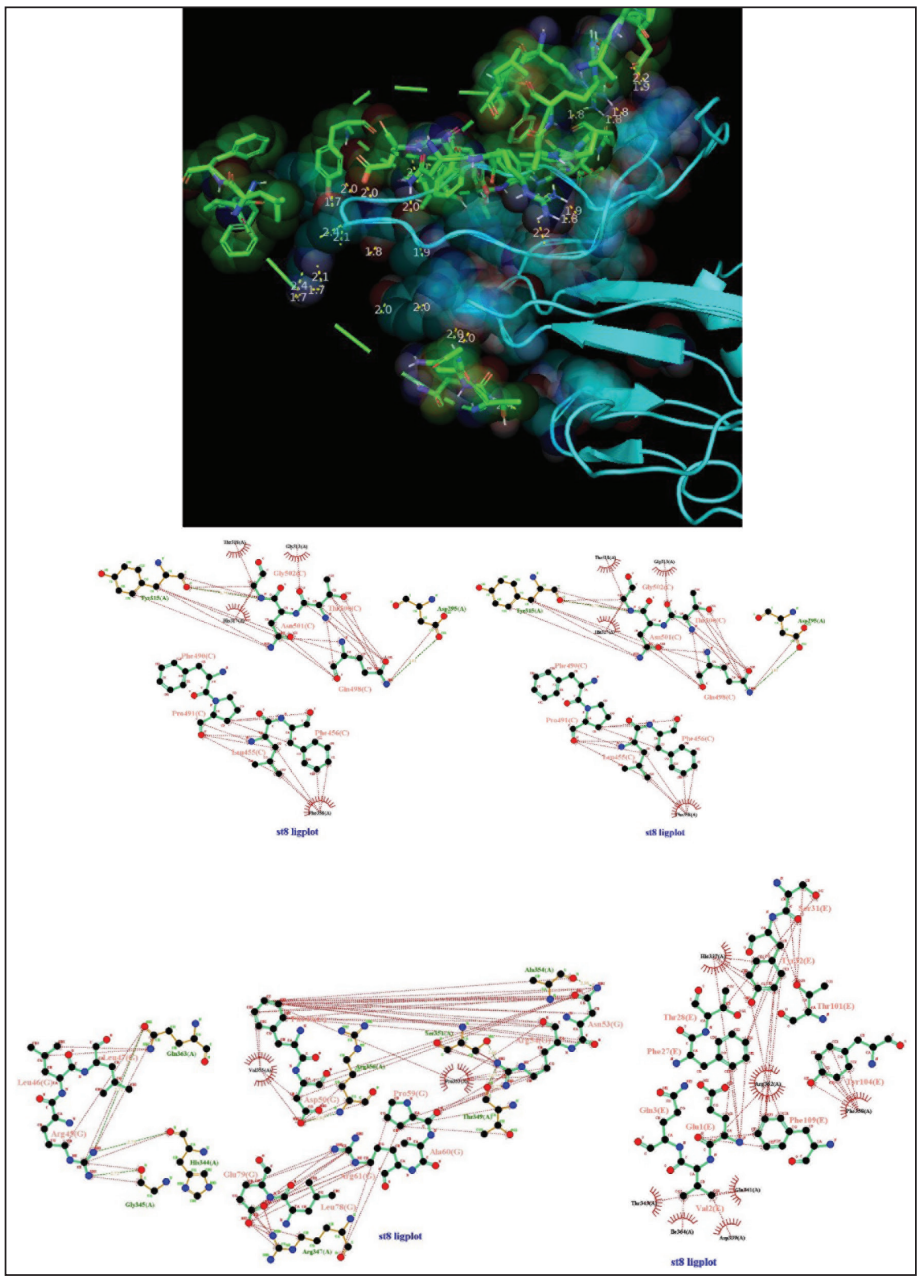

Fig. 8. Surface/glycoprotein of SARS-CoV-2 [PDB ID 7R40] with st8 (PDB ID 1A13) (wasp toxin).

ligand-protein complex under experimental conditions that mimic the cellular environment (Table 3, Fig. 14).

Discussion

For better human sustainability, it is essential to create fresher defenses against the SARS-CoV-2 virus. In an effort to combat and contain the spread of SARS-CoV-2, numerous researchers from all over the world are involved in the development of either new molecules or the remodeling of existing ones. In parallel, the aim of the present research is to find a novel life-saving treatment by evaluating the impact of scorpion, spider, and wasp toxins on the SARS-CoV-2 surface spike protein. After a thorough review of the literature, the SARS-CoV-2 surface spike protein with PDB ID: 7R40 was chosen for testing, and nine toxins with scorpion, spider, and wasp origins were chosen, as shown in Tables 1 and 2. Eight of the chosen toxins (st1, st2, st3, st4, st5, st6, st7, st8) were chosen to be processed through cluspro-2 for running

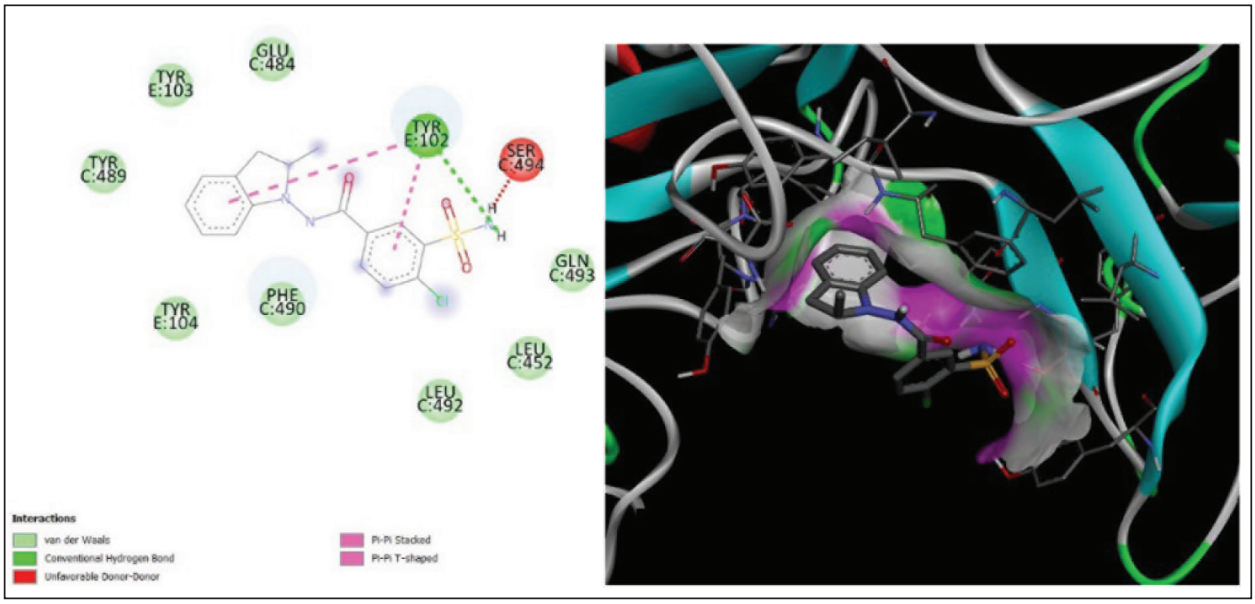

Fig. 9. Surface/glycoprotein of SARS-CoV-2 [PDB ID 7R40] with BL1 (PDB ID BL1) (scorpion toxin).

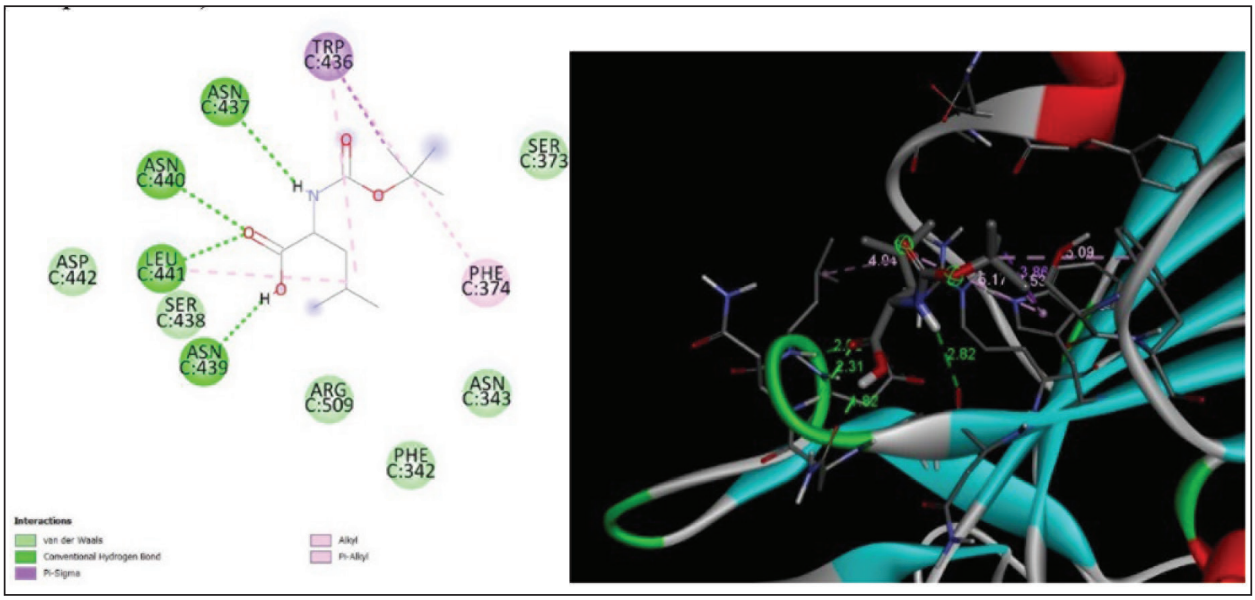

Fig. 10. Surface/glycoprotein of SARS-CoV-2 [PDB ID 7R40] with BL2 (PDB ID BL2) (scorpion toxin).

with an automated algorithm and analyzed using PyMOL because the majority of the chosen toxins were proteinaceous in nature. Five molecules (BL1, BL2, BL3, BL4, and SMP) were chosen to be tested by *PyRx v.0.8* and visualized by *BIOVIA–Discovery studios* (Chérifi and Laraba-Djebari, 2021; El Hidan *et al.*, 2021).

In the case of protein–protein interaction of the used toxins, the minimum score for hydrophobic favored—cluster scores of −2,032.4 was recorded for the st8 (wasp toxin), and the maximum score was recorded for st6 (spider toxin) −1,176.5. The minimum electrostatic favored—cluster scores of −1,451.6 was recorded for st8 (wasp toxin), and the maximum score was recorded for st6 (spider toxin) −880.9. The minimum Van der waals and electrostatic force—cluster scores of −350.1 were recorded for st8 (wasp toxin), the maximum with −194.6 was recorded for st7 (spider toxin), the minimum balanced score—cluster score of −1,416.9 was recorded for the st8 (wasp toxin), and the maximum of −829.4 was recorded for st6 (spider toxin). The interaction of wasp toxin with the target

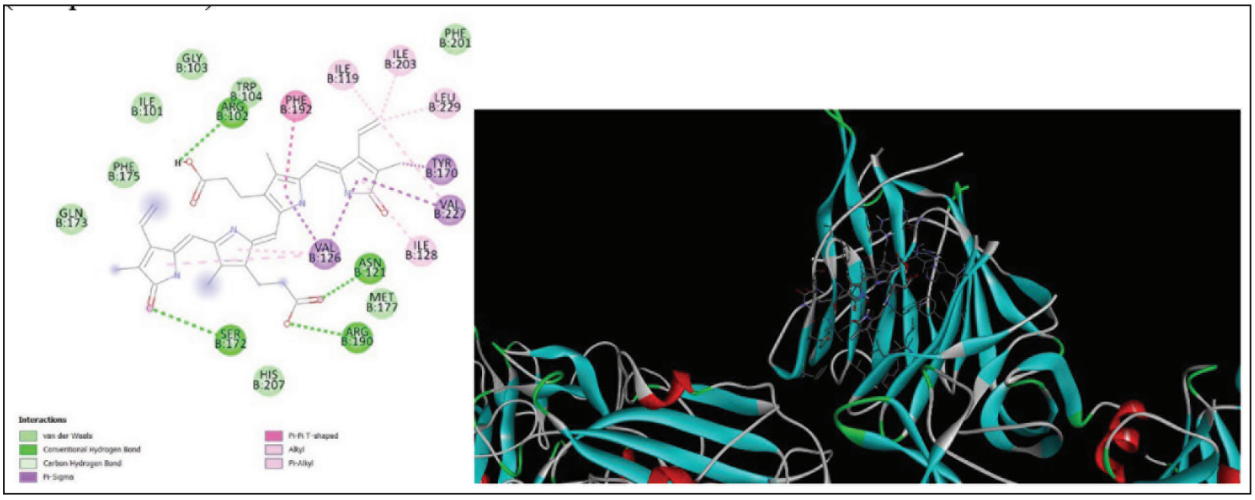

Fig. 11. Surface/glycoprotein of SARS-CoV-2 [PDB ID 7R40] with BL3 (PDB ID BL3) (scorpion toxin).

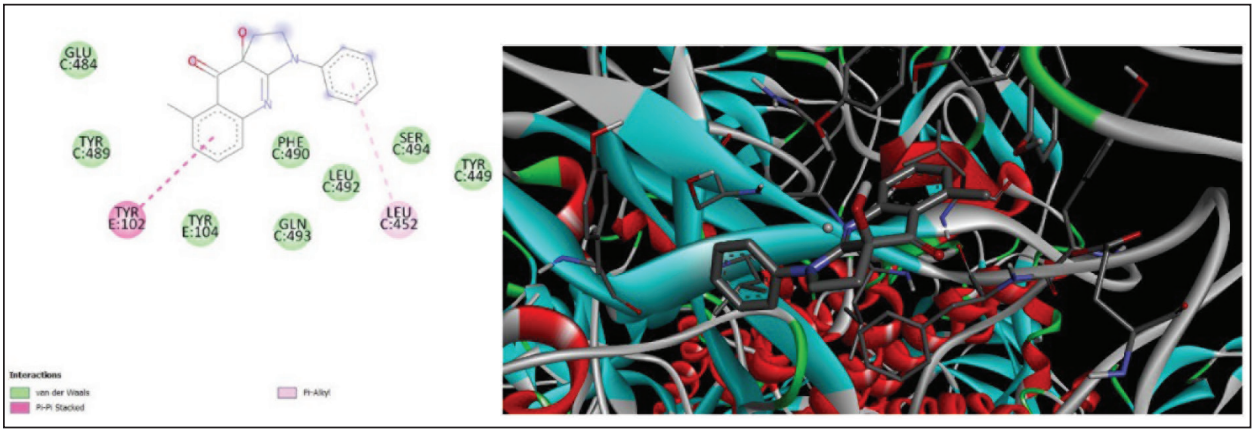

Fig. 12. Surface/glycoprotein of SARS-CoV-2 [PDB ID 7R40] with BL4 (PDB ID BL4) (scorpion toxin).

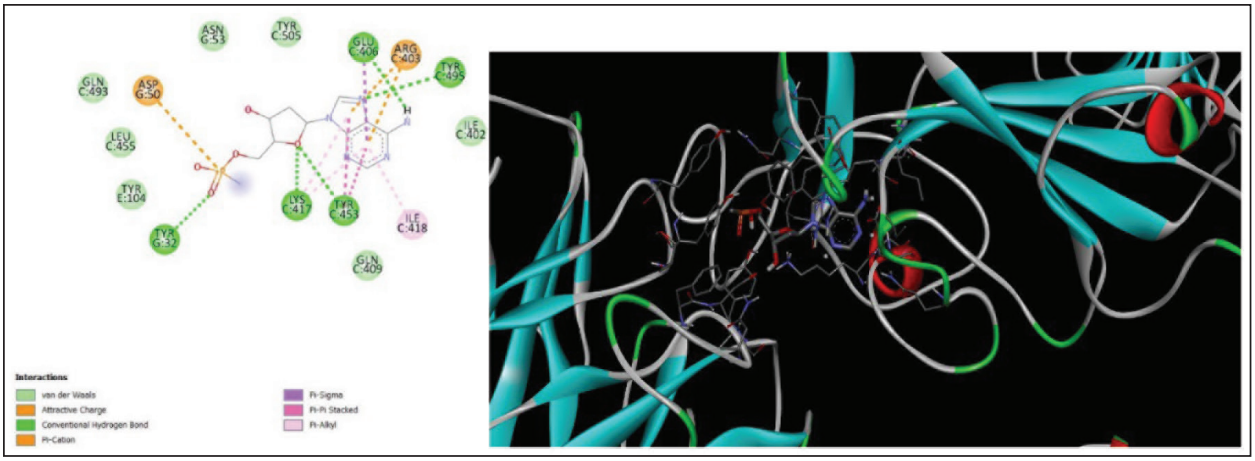

Fig. 13. Surface/glycoprotein of SARS-CoV-2 [PDB ID 7R40] with SMP (PDB ID SMP) (scorpion toxin)

protein occurred at a competitive H-bond distance of 1.7 Å (Mahnam *et al.*, 2021; Oliveira *et al.*, 2023).

Furthermore, the protein–ligand interactions were studied for five scorpion toxins specifically BL1, BL2, BL3, BL4, and SMP expressed the affinity scores of BL1: −7.8, BL2: −5, BL3: −8.3, BL4: −7.3, and SMP: −6.5 exclusively. The least affinity score was noted for BL3, and the nearest H-bond was noted for BL2 (Siniavin *et al.*, 2021).

Through this study, the wasp toxin *mastoparan* and *BL3* with great docking scores emerged as the strongest candidate for the novel medication study and development as an anti-SARS-CoV-2 agent. The remodeling of the protein in a favorable way may be useful in combating the propagation of viral infections including SARS-CoV-2. A similar attempt was published explaining beta-sitosterol obtained from natural sources can be a challenging candidate for the development of viral entry inhibitors (Viol *et al.*, 2021). Furthermore, a similar study successfully identifies the pharmacophore with the potential to disrupt the human immunodeficiency virus (HIV) glycoprotein which is the mode of entry of HIV into the cluster differentiating cells of the human immune system; in the same manner, as the HIV and SARS -CoV-2 belongs to the class of RNA viruses, the SARS-CoV-2 spike protein could be a better target to develop entry inhibitor novel molecules through molecular docking and MD simulations (Germoush *et al*., 2024) which could prove beneficial in the management of communicable infections such as SARS-CoV-2. (Easwaran *et al.*, 2024). A few manuscripts are available reflecting the need of the current research, however, not focus on the venoms but on other antiviral agents to enhance and obtain the molecule with more affinity. Therefore, the present study is appropriate for this scenario. In another study published, interferons are considered as desired candidates for the management of viral complications and infections.

The compounds of the current inquiry, eight of which are venoms but proteins, have the potential to be a dependable source of anti-SARS-CoV-2 because they are proteinaceous in origin and are very useful in the governance of viral infections, including HIV. Scorpion toxins such as BL-1,2,3,4 and SMP also showed their potency in bringing the conformational changes in SARS-CoV spike protein as similar to that of the antiviral agents which limits the entry of the virus into the healthy cells proves to be a potential candidate for future anti-SARS-CoV-2 molecules development (Muhammad Fakih *et al.*, 2022). However, Wasp toxin-Mastoparan emerges as a potent candidate for the same purpose. It is well established that the Wasp toxin-Mastoparan is an excellent agonist of GTPase which helps in the coupling of cell surface receptors to the intracellular protein components, which might result in the toxicity of the molecule as its agonist action is more potent than the antagonist on the GTPase intracellularly. Hence, future research must focus on the toxicity parameters of the mastoparan (Higashijima *et al.*, 1988), even mastoparan has revealed that if conjugated with fluvastatin has shown promising results in suppressing cancer cellular growth in conditions such as lung cancer through apoptosis and membranolytic action. It was also identified that the inflammatory mediators such as interleukins were inhibited and tumor necrosis factors were raised (Alhakamy *et al.*, 2021). A study published in the year 2013 has established that the mastoparan-derived peptide possesses the anti-viral capability and it was accordingly reported to inactivated a range of enveloped viruses in an *in vitro* model, which designates it as a broad spectrum anti-viral agent, which can play a strong role in the management of viral infections such as SARS-CoV-2 (Sample *et al.*, 2013). Similarly, the mastoparan inhibits human alphaherpesvirus and reduces its expression by over eighty percent in an *in vitro* analysis, which presents a positive prospect for the consideration of mastoparan as the potent anti-viral agent. (Vilas Boas *et al.*, 2024)

Additionally, the conformational dynamics and stability of the complex are revealed by the MD simulation of the interaction between Wasp toxin-Mastoparan and the SARS-CoV-2 spike protein. The minimal deviations shown by the ligand's RMSD (0.39–0.54 Å) and the protein's RMSD (0.026–0.34 Å) imply that both the ligand and the protein retain structural stability during the simulation. A stable folding state is supported by the radius of gyration (Rg) values, which show that the protein's compactness stays mostly constant (51.236–51.25 Å). Consistent energy levels are shown by the potential energy values (5,280,507–5,280,844), which suggests that the system is well-equilibrated. Furthermore, significant molecular interactions and surface engagement between the ligand and protein are implied by the VSA of 2,45,950–2,46,400 (Table 3 and Fig. 14). These results imply that the spike protein is a stable binding site for the Wasp toxin-Mastoparan,

Table 3. MD simulation results of ligand–protein complex using NAMD/VMD application.

Ligand	Protein	*RMSD Å*	*Radius of gyration (Rg) Å*	*Potential energy (Kcal/mol)*	*VSA*
Wasp toxin-Mastoparan	SARS-CoV-2 spike protein	Ligand: 0.39–0.54 Protein: 0.026 – 0.34	51.236–51.25	5280507–5280844	245950–246400

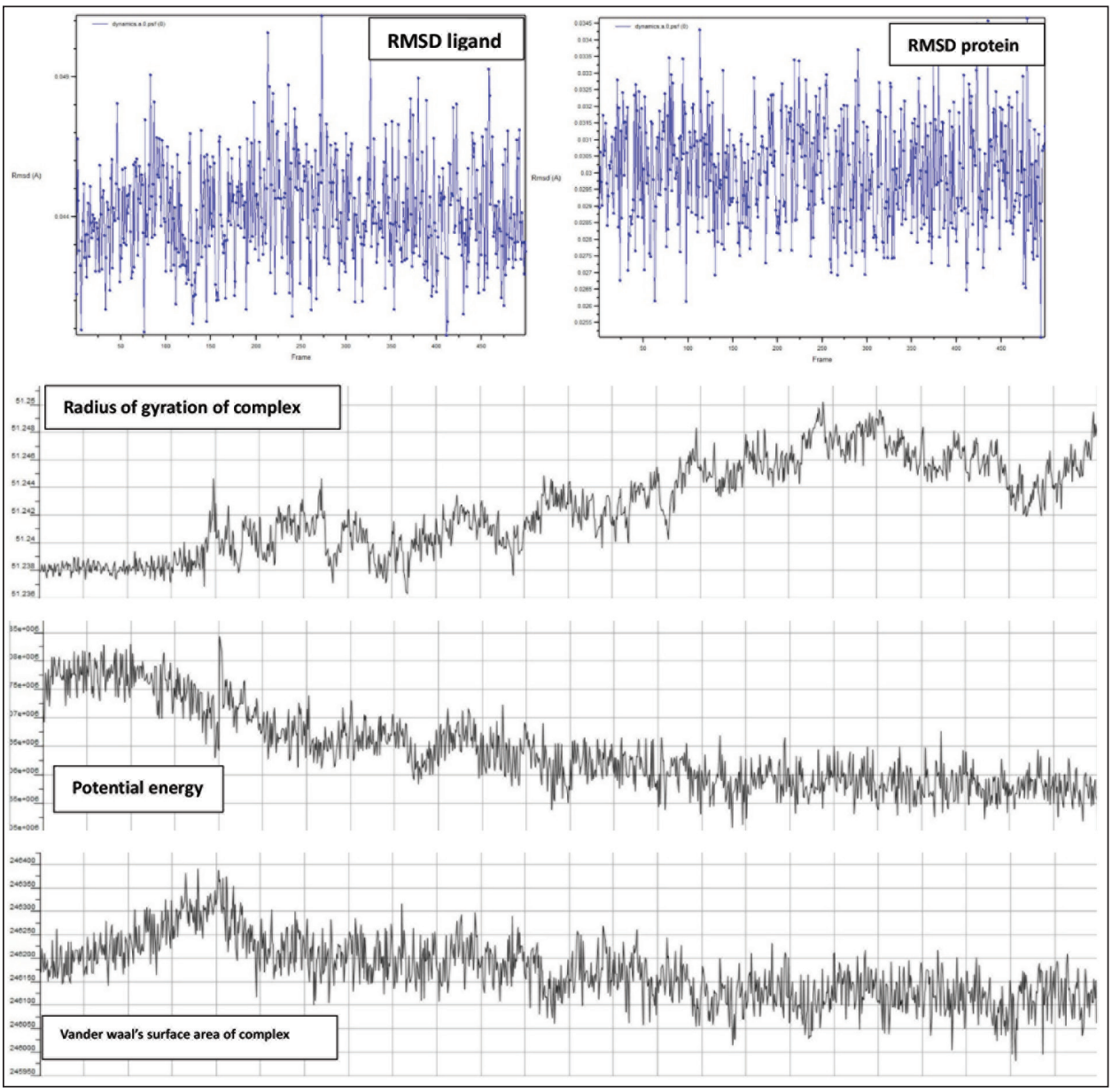

Fig. 14. Represents the RMSD graph of ligand and protein, graph of radius of gyration, potential energy, and Van der waals surface area of complex.

which makes it a highly suitable candidate for further research. Similar studies where small membrane-bound peptides were targeted for the transportation of active agents were studied, which has revealed a prospective and beneficial outcome of conjugating drugs with small membrane bound peptides where the latter facilitates the penetration of active agents into the virus-infected cells (Ivánczi *et al.*, 2023). Hence, through this study, it can be proposed that the Wasp toxin-Mastoparan is a challenging candidate for the creation of innovative anti-viral medicinal agents.

Conclusion

The SARS-CoV-2 pandemic threw a challenge for the entire scientific community. The search for treatments for the potentially fatal SARS-CoV-2 infection was started in the year 2019 and is still ongoing, new medications with antiviral properties were searched or developed without a permanent cure. Hence, through the current research, an attempt was made to identify and develop a novel potent antiviral agent derived from natural animal toxins employing promising *in silicon* approach including virtual screening, molecular docking, and MD simulation.

Animal, insect, and plant toxins are potential therapeutic antiviral candidates that could potentially treat SARS-CoV-2 infections with manageable side effects. In this regard, thirteen potential animal toxins from the scorpion, spider, and wasp species were selected and showed a variety of binding interactions with the target protein after molecular docking and the best-interacted toxin was selected for performing MD simulations to understand the stability of the complex formed. Wasp toxin "*mastoparan*" exhibited favorable interactions with SARS-CoV-2 surface-spike protein with the best affinities scores, hence can be preferred as SARS-CoV-2 surface-spike protein inhibitors. As per the molecular docking results, it binds effectively to one of the chains of the spike protein and impairs its action which could potentially inhibit the viral penetration into the healthy cells. Additionally, MD simulation of the complex formed was also studied employing NAMD/VMD tools to determine the stability and conformational changes if any have taken place post interaction and the complex resulted to be stable under stimulatory conditions resembling cellular environment. Through this *in silicon* research, it can be explained that the *mastoparan* with the best scores and other animal toxin with lower scores are to be considered for developing a successful viral entry inhibitor in humans.

Limitations

The study has several limitations that must be acknowledged. A primary limitation is the lack of experimental validation, as the findings are solely based on *in silicon* methods, including molecular docking and molecular simulation studies. These computational approaches provide valuable insights into binding affinities and interaction stabilities but cannot fully replicate the complexity of biological systems; however, MD simulations were performed under reflecting the cellular standards, and still, it needs to be validated through future studies. Additionally, the focus on structural aspects of wasp toxin and SARS-CoV-2 spike protein interaction does not address the potential immunogenicity of target effects or toxicity *in vivo*. Another limitation is the limited number of toxins analyzed, which may overlook other promising candidates with similar or superior properties. To address these gaps, future research should prioritize experimental validation through *in vitro* studies to confirm binding efficacy and inhibitory strength, followed by *in vivo* studies to assess pharmacological and toxicological efficacies. Alongside, Structural modification can be done to the active molecule to optimize the wasp toxin such as *mastoparan* for enhanced accuracy and reduced adverse effects could prove expanding the toxin library. Furthermore, employing advanced computational techniques such as quantum mechanics or molecular mechanics simulations may further refine potent candidate selection and provide deeper systematic insights.

Acknowledgment

The authors extend their appreciation to the Deanship of Scientific Research at Jouf University, Saudi Arabia, for funding this work through research grant number (DSR2022-RG-0118).

Conflicts of interest

The authors declare no conflict of interest.

Funding

This work was funded by the Deanship of Scientific Research at Jouf University under Grant Number (DSR2022-RG-0118)

Authors' contributions

MMA designed the research. MF, MJ, BA, MS, DM, NG, and SA data analysis and writing the manuscript. The manuscript revised by MOG, MF, AA, MS, and MMA. Supervision of the data analysis by MOG. Fund applied by MOG and MF. The final manuscript read, corrected, and approved by all authors.

Data availability

All data generated or analyzed during this study are included in this article.

References

Alhakamy, N.A., Ahmed, O.A.A., Md, S. and Fahmy, U.A. 2021. Mastoparan, a peptide toxin from wasp venom conjugated fluvastatin nanocomplex for suppression of lung cancer cell growth. Polymers 13(23), 4225; doi:0.3390/polym13234225.

Alhowaish, T.S., Alhamadh, M.S., Alhabeeb, A.Y., Aldosari, S.F., Masuadi, E. and Alrashid, A. 2022. Outcomes of COVID-19 in inflammatory rheumatic diseases: a retrospective cohort study. Cureus 14(6), e26343; doi:10.7759/cureus.26343.

Arzamasov, A.A., Vassilevski, A.A. and Grishin, E.V. 2014. Chlorotoxin and related peptides: Short insect toxins from scorpion venom. Russ. J. Bioorg. Chem. 40, 359–369; doi:10.1134/S1068162014040013.

Bansal, P., Kumar, R., Singh, J. and Dhanda, S. 2021. In silico molecular docking of SARS-CoV-2 surface proteins with microbial non-ribosomal peptides: identification of potential drugs. J. Proteins Proteom. 12(3), 177–184; doi:10.1007/s42485-021-00072-z.

BIOVIA, D.S. 2020. Discovery studio visualiser v.21.1.0.20298. San Diego, CA: Dassault Systèmes.

Chérifi, F. and Laraba-Djebari, F. 2021. Bioactive molecules derived from snake venoms with therapeutic potential for the treatment of thrombo-cardiovascular disorders associated with COVID-19. Protein J. 40(6), 799–841; doi: 10.1007/s10930-021-10019-4.

Dallakyan, S. and Olson, A.J. 2015. Small-molecule library screening by docking with PyRx. in Chemical Biology: Methods and Protocols. Eds., Hempel, J.E., Williams, C.H. and Hong, C.C. New York, NY: Springer New York, pp: 243–250.

Du, W., Hurdiss, D.L., Drabek, D., Mykytyn, A.Z., Kaiser, F.K., González-Hernández, M., Muñoz-

Santos, D., Lamers, M.M., van Haperen, R., Li, W., Drulyte, I., Wang, C., Sola, I., Armando, F., Beythien, G., Ciurkiewicz, M., Baumgärtner, W., Guilfoyle, K., Smits, T., van der Lee, J., van Kuppeveld, F.J.M., van Amerongen, G., Haagmans, B.L., Enjuanes, L., Osterhaus, A.D.M.E., Grosveld, F. and Bosch, B.J. 2022. An ACE2-blocking antibody confers broad neutralization and protection against Omicron and other SARS-CoV-2 variants of concern. Sci. Immunol. 7(73), eabp9312; doi:10.1126/sciimmunol.abp9312.

Easwaran, V., Alshahrani, S., Mantargi, M.J.S., Bommireddy, B., Khan, N.A., Alavudeen, S.S., Goruntla, N., Almeleebia, T., Thattarauthodiyil, U. and Awais, M. 2024. Examining factors influencing public knowledge and practice of proper face mask usage during the COVID-19 pandemic: a cross-sectional study. PeerJ 12, e16889; doi:10.7717/peerj. 16889.

El Hidan, M.A., Laaradia, M.A., El Hiba, O., Draoui, A., Aimrane, A. and Kahime, K. 2021. Scorpion-derived antiviral peptides with a special focus on medically important viruses: an update. Biomed. Res. Int. 2021, 9998420; doi:10.1155/2021/9998420.

El Sayed, S.M., Aboonq, M.S., El Rashedy, A.G., Aljehani, Y.T., Abou El-Magd, R.M., Okashah, A.M., El-Anzi, M.E., Alharbi, M.B., El-Tahlawi, R., Nabo, M.M.H., Yousef, R.S., Elshazley, M., Abu-Elnaga, M., Mahmoud, H.S., El-Alaf, H., Abdelrahman, A.I., Abdel-Gawad, A.R. and Soliman, T.M2020. Promising preventive and therapeutic effects of TaibUVID nutritional supplements for COVID-19 pandemic: towards better public prophylaxis and treatment (A retrospective study). Am. J. Blood Res. 10(5), 266–282.

Germoush, M.O., Fouda, M., Mantargi, M.J.S., Sarhan, M., Alrashdi, B.M., Massoud, D., Alzwain, S., Ghaboura, N., Altyar, A.E. and Abdel-Daim, M.M. 2024 Molecular docking of eleven snake venom peptides targeting human immunodeficiency virus capsid glycoprotein as inhibitors. Open Vet. J. 14(11), 2936–2949; doi:10.5455/OVJ.2024.v14.i11.22.

Higashijima, T., Uzu, S., Nakajima, T. and Ross, E.M. 1988. Mastoparan, a peptide toxin from wasp venom, mimics receptors by activating GTP-binding regulatory proteins (G proteins). J. Biol. Chem. 263(14), 6491–6494; doi:10.1016/S0021-9258(18)68669-7.

Hu, B., Guo, H., Zhou, P. and Shi, Z.L. 2021. Characteristics of SARS-CoV-2 and COVID-19. Nat. Rev. Microbiol. 19(3), 141–154; doi:10.1038/s41579-020-00459-7.

Humphrey, W., Dalke, A. and Schulten, K. 1996. VMD - visual molecular dynamics. J. Mol. Graphics. 14, 33–38; doi:10.1016/0263-7855(96)00018-5.

Ivánczi, M., Balogh, B., Kis, L. and Mándity, I. 2023. Molecular dynamics simulations of drug-conjugated cell-penetrating peptides. Pharmaceuticals 16(9), 1251; doi:10.3390/ph16091251.

Kozakov, D., Beglov, D., Bohnuud, T., Mottarella, S.E., Xia, B., Hall, D.R. and Vajda, S. 2013. How good is automated protein docking? Proteins 81(12), 2159–2166; doi:10.1002/prot.24403.

Kozakov, D., Hall, D.R., Xia, B., Porter, K.A., Padhorny, D., Yueh, C., Beglov, D. and Vajda, S. 2017. The ClusPro web server for protein-protein docking. Nat. Protoc. 12(2), 255–278; doi:10.1038/nprot.2016.169.

Kusunoki, H., Wakamatsu, K., Sato, K., Miyazawa, T. and Kohno, T. 1998. G Protein-bound conformation of mastoparan-X: heteronuclear multidimensional transferred nuclear overhauser effect analysis of peptide uniformly enriched with 13C and 15N. Biochemistry 37(14), 4782–4790; doi: 10.1021/bi972756p.

Laskowski, R.A. and Swindells, M.B. 2011. LigPlot+: multiple ligand–protein interaction diagrams for drug discovery. J. Chem. Inf. Model. 51(10), 2778–2786; doi: 10.1021/ci200227u.

Lees, J.A., Messa, M., Sun, E.W., Wheeler, H., Torta, F., Wenk, M.R., De Camilli, P. and Reinisch, K.M. 2017. Lipid transport by TMEM24 at ER-plasma membrane contacts regulates pulsatile insulin secretion. Science 355(6326), eaah6171; doi:10.1126/science.aah6171.

Mahnam, K., Lotfi, M. and Shapoorabadi, F.A. 2021. Examining the interactions scorpion venom peptides (HP1090, Meucin-13, and Meucin-18) with the receptor binding domain of the coronavirus spike protein to design a mutated therapeutic peptide. J. Mol. Graph Model. 107, 107952; doi:10.1016/j.jmgm.2021.107952.

Mandard, N., Sy, D., Maufrais, C., Bonmatin, J.-M., Bulet, P., Hetru, C. and Vovelle, F. 1999. Androctonin, a novel antimicrobial peptide from scorpion androctonus Australis: solution structure and molecular dynamics simulations in the presence of a lipid monolayer. J. Biomol. Struct. Dyn. 17(2), 367–380; doi:10.1080/07391102.1999.10508368.

Meng, L., Zhao, Y., Qu, D., Xie, Z., Guo, X., Zhu, Z., Chen, Z., Zhang, L., Li, W., Cao, Z., Tian, C. and Wu, Y. 2020. Ion channel modulation by scorpion hemolymph and its defensin ingredients highlights origin of neurotoxins in telson formed in Paleozoic scorpions. Int. J. Biol. Macromol. 148, 351–363; doi:10.1016/j.ijbiomac.2020.01.133.

Mudenda, S., Mukosha, M., Mwila, C., Saleem, Z., Kalungia, A.C., Munkombwe, D., Daka, V., Witika, B.A., Kampamba, M., Hikaambo, C.N., Sadiq, M.J., Chileshe, M., Kasanga, M., Mufwambi, W., Mfune, R.L., Matafwali, S.K., Masebe, P.O., Muungo, L.T., Bwalya, A.G., Kampamba, R.M., Zingani, E., Banda, D.C., Sintema, E.J., Gupta,

A., Abdulrahman, N.M., Hangoma, J.M., Phiri, M.N., Hang'andu, D., Ngazimbi, M., Mudenda, F., Banda, M. and Kazonga, E. 2021b. Impact of the coronavirus disease on the mental health and physical activity of pharmacy students at the University of Zambia: a cross-sectional study. Int. J. Basic Clin. Pharmacol. 10(4), 324–332; doi:10.18203/2319-2003.ijbcp20211010.

Mudenda, S., Witika, B., Sadiq, M.J., Banda, M., Mfune, R.L., Daka, V., Kalui, D, Phiri, M., Kasanga, M., Mudenda, F. and Mufwambi, W. 2021a. Self-medication and its consequences during & after the coronavirus disease 2019 (COVID-19) pandemic: a global health problem. Eur. J. Env. Public Hlt. 1, em0066; https://doi.org/10.29333/ejeph/9308

Muhammad Fakih, T., Luthfika Dewi, M. and Syahroni, E. 2022. The inhibition of angiotensin-converting enzyme 2 receptors of SARS-CoV-2 through mucroporin derived from scorpion venom. KnE Life Sci. 7(5), 92–102; doi:10.18502/kls.v7i5.12514

Odoemelam, C.S., Hunter, E., Simms, J., Ahmad, Z., Chang, M.-W., Percival, B., Williams, I.H., Molinari, M., Kamerlin, S.C.L. and Wilson, P.B. 2022. *In silico* ligand docking approaches to characterise the binding of known allosteric modulators to the glucagon-like peptide 1 receptor and prediction of ADME/Tox properties. Appl. Biosci. 1(2), 143–162; doi:10.3390/applbiosci1020010.

Oliveira, I., Ferreira, I., Jacob, B., Cardenas, K., Cerni, F., Baia-da-Silva, D., Arantes, E., Monteiro, W. and Pucca, M. 2023. Harnessing the power of venomous animal-derived toxins against COVID-19. Toxins 15(2), 159; doi:10.3390/toxins15020159.

Reis, P.V.M., Boff, D., Verly, R.M., Melo-Braga, M.N., Cortés, M.E., Santos, D.M., Pimenta, A.M.d.C., Amaral, F.A., Resende, J.M. and de Lima, M.E. 2018. LyeTxI-b, a synthetic peptide derived from lycosa erythrognatha spider venom, shows potent antibiotic activity *in Vitro* and *in Vivo*. Front. Microbiol. 9, 667; doi:10.3389/fmicb.2018.00667.

Salahshoori, I., Mobaraki-Asl, N., Seyfaee, A., Mirzaei Nasirabad, N., Dehghan, Z., Faraji, M., Ganjkhani, M., Babapoor, A., Shadmehr, S.Z. and Hamrang, A. 2021. Overview of COVID-19 disease: virology, epidemiology, prevention diagnosis, treatment, and vaccines. *Biologics* 1(1), 2–40; doi:10.3390/biologics1010002

Sample, C.J., Hudak, K.E., Barefoot, B.E., Koci, M.D., Wanyonyi, M.S., Abraham, S., Staats, H.F. and Ramsburg, E.A. 2013. A mastoparan-derived peptide has broad-spectrum antiviral activity against enveloped viruses. Peptides 48, 96–105; doi:10.1016/j.peptides.2013.07.014.

Schrödinger, LLC. (2015). The PyMOL molecular graphics system, Version 1.8. Schrödinger, LLC, New York, NY, USA.

Siniavin, A.E., Streltsova, M.A., Nikiforova, M.A., Kudryavtsev, D.S., Grinkina, S.D., Gushchin, V.A., Mozhaeva, V.A., Starkov, V.G., Osipov, A.V., Lummis, S.C.R., Tsetlin, V.I. and Utkin, Y.N. 2021. Snake venom phospholipase A2s exhibit strong virucidal activity against SARS-CoV-2 and inhibit the viral spike glycoprotein interaction with ACE2. Cell Mol. Life Sci. 78, 7777–7794; doi:10.1007/s00018-021-03985-6.

Vajda, S., Yueh, C., Beglov, D., Bohnuud, T., Mottarella, S.E., Xia, B., Hall, D.R. and Kozakov, D. 2017. New additions to the ClusPro server motivated by CAPRI. Proteins 85(3), 435–444; doi:10.1002/prot.25219.

Vassilevski, A.A., Fedorova, I.M., Maleeva, E.E., Korolkova, Y.V., Efimova, S.S., Samsonova, O.V., Schagina, L.V., Feofanov, A.V., Magazanik, L.G. and Grishin, E.V. 2010. Novel class of spider toxin: active principle from the yellow sac spider *Cheiracanthium punctorium* venom is a unique two-domain polypeptide. J. Biol. Chem. 285(42), 32293–32302; doi:10.1074/jbc.M110.104265.

Vilas Boas, L.C.P., Buccini, D.F., Berlanda, R.L.A., Santos, B.d.P.O., Maximiano, M.R., Lião, L.M., Gonçalves, S., Santos, N.C. and Franco, O.L. 2024. Antiviral activities of mastoparan-L-derived peptides against human alphaherpesvirus 1. Viruses 16(6), 948; doi:10.3390/v16060948

Viol, D.K., Arif, N.M.A., Farida, A.D., Wahyu, C.R., Tim, G.A.D., Rahadian, Z. and Alexander, P.N. 2021. Molecular docking and dynamic simulation of entry inhibitor from *Tamarindus indica* bioactive compounds against SARS-CoV-2 infection via viroinformatics study. Biochem. Cell. Arch. 21(2), 3323–3327.